# Viewperiod Generator for Spacecraft and the Planets

W. D. Diemer
Network Operations Office

*This article describes a method, and the supporting software, developed to provide an inexpensive means of generating spacecraft and planetary viewperiods for the Deep Space Stations over a long period of time. In the past, the only method for obtaining this information was an expensive and complex computer program which provided these data as a secondary output to the actual station look angles.*

The task of receiving and transmitting signals from and to spacecraft in solar orbits poses many observational problems which are unlike those of conventional astronomy.

Conventional telescopes are most frequently targeted on stellar objects whose positions are fixed on the celestial spheres. Less often, they are aimed at planets and other objects within the solar system, whose varying positions in the heavens are known with great accuracy for long into the future.

In contrast, tracking antennae are targeted most frequently on spacecraft whose paths across the sky can only be estimated in advance of launch. Once aloft and en route, their paths can be determined with sufficient accuracy for tracking purposes by using not only the laws of celestial mechanics but also those of propulsion physics. Unlike natural objects, their trajectories can be altered on command to achieve desired observational objectives.

As a consequence of these uncertainties in spacecraft trajectories, it is more difficult to make long-range plans for efficient use of the tracking antenna in the NASA Deep Space Network (DSN) operated by the Jet Propulsion Laboratory (JPL).

The efficient use of these expensive scientific instruments requires that long-range planners have reasonably accurate estimates of the times during which particular spacecraft will be in view (i.e., above the horizon) for long periods into the future. With these data, they can determine whether two spacecraft are in view during the same period, during overlapping periods, or during non-overlapping periods. (The word *view* must be interpreted here in a radio sense rather than in an optical sense.) If two spacecraft of interest are above the horizon during the same period, but not within the beam width of one antenna, then only one can be tracked on a given day by a given station (though, of course, it is possible to use a portion of the "viewperiod" for each, rather than devoting the entire period to one and ignoring the other). On the other hand, if two spacecraft have non-overlapping viewperiods, the antenna can be aimed at the second after the first has set.

Such information (i.e., the rise and set times for each spacecraft at each station) also reflects back on other planning activities. The projected workloads developed by long-range planners may influence budgetary allocations and requests in future years, as well as manpower loading, equipment requests, and maintenance and training needs. For several years, the Jet Propulsion Laboratory has been using two partial solutions to this problem: highly accurate short-range predictions and approximate long-range predictions.

Every few days, a computer run is performed which generates precise aiming coordinates for use in tracking particular spacecraft from each station. This program, constructed on iterative principles, produces coordinates for five-minute intervals throughout the day. Rise and set times are only one of the products of these calculations. This program, known as PREDIX, is very time-consuming and expensive to operate; it requires nearly one hour of computer time (IBM 360/75) to generate two weeks of aiming coordinates. Because of convenience and need for frequency updates, these programs are rarely executed more than a few weeks in advance of need, as the results are used for actual tracking and must be as accurate as possible.

For longer future projections, a semi-graphical method has been used. JPL's Navigation and Mission Design Section has the responsibility for developing approximate trajectories and alternatives for proposed missions and maintaining accurate flight paths for vehicles already launched, using actual positional fixes. This section has developed a digital plot program, using both the Univac 1108 and a Calcomp Plotter. The output of this program (Fig. 1) is a graph containing three superimposed plots. All plots use time as one dimension, along the length of the continuous forms, so that trajectories of any time span can be shown. The other dimensions are:

(1) *Declination*—the angular distance between the spacecraft and the celestial equator. This variable almost always has values ranging between $-25°$ and $+25°$, since to date all spacecraft have been directed in orbits close to the ecliptic.

(2) *Range*—the distance from the Earth to the spacecraft. Since all spacecraft launched to date (except Pioneer 10) have had orbits not farther than that of the planet Mars, this variable usually ranges between zero and 400 million kilometers. This value can be used directly to calculate round-trip signal times at the speed of light.

(3) *Local Meridian Crossing Time*—the time at which the spacecraft crosses the local meridian at the observing station. (The meridian is the line that bisects the sky as seen from any point on Earth. It starts at the north horizon, passes through the zenith, and ends at the south horizon.) The point at which any celestial object crosses the local meridian, as Earth rotates, is also the point of maximum elevation. It is rising from the horizon until it crosses the meridian; thereafter its elevation decreases until it sets. This variable can have any value between zero and 24 hours. Objects that are close to a celestial pole never rise nor set. If they are in the same hemisphere as the observing station, they trace a circle in the sky around the pole, crossing the meridian twice each day. The higher crossing is termed the superior crossing, the other is the inferior crossing. Conversely, objects close to the pole opposite the observing station never rise at all. Their circles in the sky never reach above the horizon. To date, no spacecraft have been sent in orbits so close to the poles that they are in constant view (or constant eclipse) from any station.

Using these plots as a starting point, we have developed a computer method for generating rise and set times for any spacecraft, as viewed from any point on Earth, for any period and as far into the future as trajectories have been calculated. This program can produce these times for every single day, if desired. For practical purposes, however, it is usually sufficient to produce them at weekly or monthly intervals, since the day-to-day changes are quite small (2–5 minutes), and may be determined by interpolation when closer intervals are required.

In addition to the data from these plots, two other data inputs are required: the geocentric coordinates of each station (i.e., latitude and longitude on Earth's surface), and the profile of the local horizon around each station.

The phrase that JPL uses to describe this local horizon profile is "horizon mask," the term implying that a celestial object is masked from view (whether visual or radio) until it rises above the surrounding hills and mountains. This horizon mask is most conveniently represented graphically by a chart termed a "stereographic projection" (see Fig. 2).

This chart is representative of the charts developed for each station. The outer circle represents the entire sky as seen from the observation point. The shaded area around the circumference of the circle represents that portion of the sky which is not visible due to the neighboring hills, and shows the irregularity characteristic of natural topographic features. The numerous intersecting lines, circles and arcs on the chart represent the two different coordinate systems used for celestial observation. One of these systems is Earth-centered, the other is sky-centered.

Though these charts do represent the entire visible sky as seen from each of the stations in the DSN, they include some portions of the celestial sphere which are outside the observational range of the antennae. These further restrictions on viewing are a consequence of the manner in which the antennae are supported, and moved to compensate for the apparent motion of the spacecraft across the sky as Earth rotates.

These mechanical limitations on spacecraft tracking are shown on the stereographic projections represented in Fig. 2. The heavy blocked line around the figure indicates the tracking limits. The small arc near the celestial pole indicates that celestial objects close to that pole cannot be observed throughout the 24 hours. The jagged balance of this line, generally outside the circle, indicates that in these regions the antenna can be pointed below the horizon–or actually at the ground.

We shall now use the stereographic projection in Fig. 2 to illustrate the principles upon which our viewperiod generator computer program was constructed.

Let us start with an object whose declination is 0°, i.e., it lies precisely on the celestial equator. If we examine the chart closely, we see that the equator crosses the horizon mask about 1° from the eastern horizon, or 89° from the meridian. Since Earth rotates a full 360° in one day, a point on the celestial sphere seems to move equally 360° in a day, or, most simply, it takes four minutes for an object to move 1°. We therefore determine that the object will rise above the horizon (if it is on the equator) 5 hours and 56 minutes before it crosses the meridian (89° × 4 minutes = 356 minutes = 5h 56m). Similarly, we observe that the celestial equator crosses the western horizon mask exactly at sea level. The object will therefore remain in view while Earth rotates 90°. We thus determine that the object will set 6h 0m after it crosses the meridian. The total view-period duration will be the sum of these two times, or 11h 56m. The actual local times of rise and set are determined by subtracting and adding these two time intervals to the time of local meridian crossing. For example, if the object crosses the meridian at 09:52 local time, its rise is at 03:56 and its set is at 15:52.

However, local times are not adequate for the operation of the DSN. Being a worldwide operation, it must use a uniform time standard for all its stations, and has selected Greenwich Mean Time (GMT) as that standard. The local time can be easily converted to GMT by adding or subtracting the time required for Earth to rotate from the Greenwich meridian to the local meridian, which time is a direct function of the longitude of the station. Since DSS 12 is approximately 118° west of the Greenwich meridian, its time difference from GMT is 7h 52m. Therefore, the GMT rise time for the above example is 20:04 of the previous day, its GMT set time is 08:00 of the same day.

For a second example, let us choose an object whose declination is −24°, or 24° south of the celestial equator. Examining the stereographic chart, we see that at this declination, the angular distance from the meridian to the eastern horizon mask is 72°. The time equivalent of this angle is 4h 48m (72° × 4m = 288m = 4h 48m). Similarly, the angular distance from the meridian to the western horizon is 65°, and its time equivalent is 4h 20m. The duration of the viewperiod is the sum of these two, or 9h 8m. Note that this viewperiod is substantially shorter than for an object at the celestial equator. Also note that an object whose declination is greater than 48° south does not rise above the horizon at all.

For a final example, let us choose an object whose declination is +10°, or north of the celestial equator. The chart shows that the angular distance between the meridian and the eastern horizon is 100°, for a time equivalent of 6h 40m. However, we also observe that this declination arc intersects the heavy line representing the mechanical limits imposed by the HA–dec mounting of the antenna. The angular distance from the meridian to this limit is only 90°, for a time equivalent of 6h 0m. This difference illustrates the fact that, for celestial objects at this declination, observation cannot begin when the object rises above the horizon, but must wait until it comes within pointing range of the antenna, some 40 minutes later. Assuming, again, a local meridian crossing time of 09:52, such an object rises above the horizon at 03:12, but cannot be observed until 03:52. Similarly, the angular distance along the $+10°$ declination arc from the meridian to the western horizon is 97°, for a time equivalent of 6h 27m. Again, the mechanical limits imposed by the mounting restrict the actual viewing angle to 90° or 6h 0m. (Note that at high declinations, the angular distances east and west are equal. This is a consequence of the fact that the mounting is symmetrical.) Thus the object passes out of practical viewing range some 27 minutes before it actually drops below the horizon.

These three examples illustrate the three variables required to calculate local rise and set times:

(1) The time of the local meridian crossing.

(2) The declination of the object.

(3) The angular distance along the declination arc from the meridian to each horizon, or to the mechanical antenna limits in extreme latitudes.

A fourth variable, the longitude of the station, is all that is further required to convert these local times to GMT.

An interesting aspect of this approach to the solution of determining long-range rise and set times is the fact that the local meridian crossing time is the same for all stations, regardless of longitude. We are aware that when the Sun crosses the local meridian, it is local noon. Another celestial object on the Sun's meridian will also cross the local meridian at local noon. An object (say the moon whose angular distance is 30° in advance of the Sun's meridian will cross the local meridian 2 hours in advance of noon, or 10:00. And any object whose angular distance from the Sun's meridian is known will cross the local meridian at a time before or after noon, which is a direct function of the time equivalent of that angular distance.

This point must not be taken too literally. The position of an object on the celestial sphere does vary slightly from day to day. For a stellar object, this variation is the difference between a solar day and a sidereal day, or about 4 minutes. For an object pursuing a solar orbit in the same direction as Earth (i.e., a spacecraft), this variation is somewhat less. For Pioneer 10, it is about 2.5 minutes. For objects pursuing a solar orbit within Earth's orbit, the variation is somewhat greater than 4 minutes per day. As a consequence, the local meridian crossing time of a spacecraft is not precisely identical for all stations in the DSN, but the difference is seldom more than a minute or two. This variation is not of sufficient significance to affect long-range planning data, and this refinement has not been included in the program we have developed.

The declination of a celestial object also varies slightly from day to day, though this variation is even smaller than the variations in local meridian crossing time. If we again examine the sterographic projection in Fig. 2, we see that as an object moves from one declination level to another, the angular distance along the declination arc from the meridian to the horizon increases as the object approaches the pole, and decreases as it recedes from the pole. The observational consequence is that the viewperiod lengthens as the object approaches the pole, and decreases as it recedes.

If there were an object in the solar system whose position was fixed, its declination would vary as the Earth made its annual trip around the Sun, reaching a maximum of about $+23°$ at one point in the year, and a minimum of $-23°$ six months later. There is, of course, no such stationary object. The nearest approximation is the planet Pluto, whose annual motion across the sky is somewhat less than 2°, since it requires 248 Earth years to complete its single solar circuit. Thus, the declination plot (see Fig. 1) of the planet Pluto would show a cycle of about 367 days, just slightly more than a year. The nearer superior planets (Neptune, Uranus, Saturn, Jupiter, and Mars) would have declination plots showing progressively larger cycles: almost 400 days for Jupiter and over 600 days for Mars. The two inferior planets (Venus and Mercury) speed around the Sun much faster than Earth. Their declination plots show cycles of much less than a year: about 200 days for Venus and about 100 days for Mercury.

The declination plots of the planets are not precisely repeated in each cycle. The nominal maximum and minimum values of $+23°$ and $-23°$ are for objects which are precisely in the ecliptic, the plane of Earth's orbit. All the planets have orbits whose planes are inclined at varying (though small) degrees to the ecliptic. The actual plots over long periods may show variations as great as $+30°$ to $-30°$ or as little as from $+16°$ to $-16°$. The declination pattern is never precisely repeated, since the revolution times of all the planets are incommensurable with Earth's year. This cyclical variation in local meridian crossing time and declination should be kept in mind when interpolating values from the tables we have produced.

Interpolation will provide rise and set times with errors usually less than those inherent in the approximate method used. These errors will be smallest when the declination plot is straight or nearly so. They will be largest when the plot is sharply curved, i.e., near the times of maximum and minimum declination. Interpolations will show the largest errors for plots which oscillate rapidly (those of Mercury and Venus) and the smallest for the slowly oscillating plots, particularly Mars.

The computer program has been designed to provide rise and set times for any object anywhere in the celestial sphere, i.e., for any object with a declination between $-90°$ (south celestial pole) and $+90°$ (north celestial pole). Since the horizon mask at each station varies irregularly, the program includes a set of tables for each station defining this mask. Table 1 is a sample set for DSS 12. It gives, for each degree of declination, the angular distance to the east and to the west horizon masks. These values were obtained by visual scaling from the stereographic projection shown in Fig. 2. Note that the table gives zero values for declinations between $-90°$ and $-49°$, indicating that celestial objects at these southern latitudes can never be viewed from Goldstone. Between $-48°$ and $+81°$, the table shows gradually increasing values (sharply at first, then more slowly), indicating that as an object climbs northward, its viewperiod lengthens. Above $+16°$ to $81°$, the values are constant, indicating that in this range, the mechanical antenna limits rather than the topographic horizon determine the bounds of the viewperiod. Finally, from $+82°$ to $+90°$, the values revert to zero, indicating that the polar mounting of the antenna prevents aiming it this close to the north celestial pole.

The accuracy of this table is limited by the scale of the stereographic projection from which it was derived. We have used one degree as our scale interval, which corresponds to a time interval of 4 minutes. The accuracy of our calculations is thus on the order of $\pm 2$ minutes, perhaps more if the actual declination is between scale points. This accuracy can, of course, be improved if declination points were chosen more closely than one degree, and if the declination arcs are measured to a finer degree of accuracy than one degree.

Though this table lookup feature can be used to determine viewperiods for the az–el stations as well as the HA–dec stations, the horizon mask of the former is amenable to a straightforward mathematical solution rather than a table lookup. The declination arc of a celestial object is part of a small circle on the celestial sphere, parallel to the great circle that is its equator. The length of this arc ($\beta$) is a function of three angles:

(1) $\lambda$, the latitude of the station

(2) $\delta$, the declination of the object

(3) $\beta$, the minimum elevation for observation (the DSN uses 6°) and can be found by a trigonometric analysis of the sphere:

$$\cos \beta = \frac{\sin \beta}{\cos \delta \cos \lambda} - \tan \delta \tan \lambda$$

This equation is used to determine rise and set times at the three 64-m Deep Space Stations. Since it is an exact formula, the rise and set times at these stations are not subject to the table lookup errors of the times at the other stations.

Data are input to the program via a card deck. Each card contains:

(1) Date.

(2) Local meridian crossing time.

(3) Declination.

From each card, the program computes the local rise and set times at each station, using either table lookup or trignometric formula as appropriate. These are then converted to GMT using the station longitude. This array is then printed out, along with the date.

This logic is repeated for each data card until the entire deck is read. Thus, the date intervals may be regular or irregular. Also, the cards may be in order, though any order other than strictly chronological would be confusing to a user.

A sample input data deck listing is shown in Table 2, and a sample output listing is shown in Table 3. The first three columns of the output simply repeat the input, for visual verification in situations where there is suspicion of error.

We are continuing to develop this program to increase its speed, economy, timeliness, and accuracy. We are adapting the trajectory program which now produces the declination and local meridian crossing plots, to produce digital output in a form suitable for input to this program. This step will save the time now required to read and interpolate the plots, and reduce the possibility of error in transferring these data to punched cards. When this step is completed, it will be necessary only to enter basic trajectory parameters (position, velocity, and acceleration) and have the computer generate declinations and local meridian crossing times first at specified intervals and then the viewperiods themselves.

Somewhat further downstream, we would like to develop the capability of showing these plots graphically, rather than numerically, on a remote terminal display. It will then be possible to punch a few buttons to identify the time period, station(s), and spacecraft and get an instant visual display of conflicts and overlaps.

Though this program was developed primarily to support the spacecraft tracking responsibilities of the DSN, it appears to have broader uses. Other radio astronomy sensors at other locations around the globe can use it to generate their own viewperiods for planetary and even stellar objects.

Optical astronomy may be able to use the program, after modifying it to include periods of darkness and daytime for similar planning of their observing schedules. Such modifications would be particularly useful, where

(1) The observatory has a non-uniform horizon mask.

(2) Atmospheric conditions prevent adherence to a planned schedule, and instant readjustments must be made.

**Table 1. Sample horizon mask for DSS 12**

| Declination | Rise | Set | Declination | Rise | Set | Declination | Rise | Set |
|---|---|---|---|---|---|---|---|---|
| −90 | 0 | 0 | −30 | 67 | 59 | 30 | 94 | 95 |
| −89 | 0 | 0 | −29 | 68 | 60 | 31 | 94 | 95 |
| −88 | 0 | 0 | −28 | 70 | 61 | 32 | 94 | 95 |
| −87 | 0 | 0 | −27 | 70 | 62 | 33 | 94 | 95 |
| −86 | 0 | 0 | −26 | 70 | 64 | 34 | 94 | 95 |
| −85 | 0 | 0 | −25 | 72 | 64 | 35 | 94 | 95 |
| −84 | 0 | 0 | −24 | 72 | 65 | 36 | 94 | 95 |
| −83 | 0 | 0 | −23 | 73 | 66 | 37 | 94 | 95 |
| −82 | 0 | 0 | −22 | 75 | 67 | 38 | 94 | 95 |
| −81 | 0 | 0 | −21 | 76 | 68 | 39 | 94 | 95 |
| −80 | 0 | 0 | −20 | 76 | 70 | 40 | 94 | 95 |
| −79 | 0 | 0 | −19 | 76 | 71 | 41 | 94 | 95 |
| −78 | 0 | 0 | −18 | 77 | 72 | 42 | 94 | 95 |
| −77 | 0 | 0 | −17 | 77 | 72 | 43 | 94 | 95 |
| −76 | 0 | 0 | −16 | 77 | 73 | 44 | 94 | 95 |
| −75 | 0 | 0 | −15 | 78 | 74 | 45 | 94 | 95 |
| −74 | 0 | 0 | −14 | 78 | 75 | 46 | 94 | 95 |
| −73 | 0 | 0 | −13 | 80 | 76 | 47 | 94 | 95 |
| −72 | 0 | 0 | −12 | 81 | 77 | 48 | 94 | 95 |
| −71 | 0 | 0 | −11 | 82 | 79 | 49 | 94 | 95 |
| −70 | 0 | 0 | −10 | 82 | 80 | 50 | 94 | 95 |
| −69 | 0 | 0 | −9 | 83 | 81 | 51 | 94 | 95 |
| −68 | 0 | 0 | −8 | 83 | 82 | 52 | 94 | 95 |
| −67 | 0 | 0 | −7 | 84 | 83 | 53 | 94 | 95 |
| −66 | 0 | 0 | −6 | 85 | 84 | 54 | 94 | 95 |
| −65 | 0 | 0 | −5 | 85 | 84 | 55 | 94 | 95 |
| −64 | 0 | 0 | −4 | 86 | 85 | 56 | 94 | 95 |
| −63 | 0 | 0 | −3 | 86 | 85 | 57 | 94 | 95 |
| −62 | 0 | 0 | −2 | 88 | 86 | 58 | 94 | 95 |
| −61 | 0 | 0 | −1 | 89 | 87 | 59 | 94 | 95 |
| −60 | 0 | 0 | 0 | 89 | 90 | 60 | 94 | 95 |
| −59 | 0 | 0 | 1 | 90 | 90 | 61 | 94 | 95 |
| −58 | 0 | 0 | 2 | 90 | 90 | 62 | 94 | 95 |
| −57 | 0 | 0 | 3 | 90 | 90 | 63 | 94 | 95 |
| −56 | 0 | 0 | 4 | 90 | 90 | 64 | 94 | 95 |
| −55 | 0 | 0 | 5 | 90 | 90 | 65 | 94 | 95 |
| −54 | 0 | 0 | 6 | 90 | 90 | 66 | 94 | 95 |
| −53 | 0 | 0 | 7 | 90 | 90 | 67 | 94 | 95 |
| −52 | 0 | 0 | 8 | 90 | 90 | 68 | 94 | 95 |
| −51 | 0 | 0 | 9 | 90 | 90 | 69 | 94 | 95 |
| −50 | 0 | 0 | 10 | 90 | 90 | 70 | 94 | 95 |
| −49 | 0 | 0 | 11 | 90 | 90 | 71 | 94 | 95 |
| −48 | 40 | 7 | 12 | 90 | 90 | 72 | 94 | 95 |
| −47 | 43 | 30 | 13 | 90 | 90 | 73 | 94 | 95 |
| −46 | 44 | 31 | 14 | 90 | 90 | 74 | 94 | 95 |
| −45 | 45 | 32 | 15 | 90 | 90 | 75 | 94 | 95 |
| −44 | 46 | 34 | 16 | 94 | 95 | 76 | 94 | 95 |
| −43 | 48 | 37 | 17 | 94 | 95 | 77 | 94 | 95 |
| −42 | 50 | 40 | 18 | 94 | 95 | 78 | 94 | 95 |
| −41 | 51 | 42 | 19 | 94 | 95 | 79 | 94 | 95 |
| −40 | 52 | 43 | 20 | 94 | 95 | 80 | 94 | 95 |
| −39 | 54 | 45 | 21 | 94 | 95 | 81 | 94 | 95 |
| −38 | 56 | 47 | 22 | 94 | 95 | 82 | 0 | 0 |
| −37 | 58 | 50 | 23 | 94 | 95 | 83 | 0 | 0 |
| −36 | 60 | 52 | 24 | 94 | 95 | 84 | 0 | 0 |
| −35 | 61 | 52 | 25 | 94 | 95 | 85 | 0 | 0 |
| −34 | 63 | 52 | 26 | 94 | 95 | 86 | 0 | 0 |
| −33 | 64 | 53 | 27 | 94 | 95 | 87 | 0 | 0 |
| −32 | 65 | 56 | 28 | 94 | 95 | 88 | 0 | 0 |
| −31 | 66 | 58 | 29 | 94 | 95 | 89 | 0 | 0 |
| −30 | 67 | 59 | 30 | 94 | 95 | 90 | 0 | 0 |

Table 2. Sample input data deck listing

| | |
|---|---|
| 72 227PN-F | 90-15 |
| 72 327PN-F | 43-32 |
| 72 426PN-F | 20-29 |
| 72 525PN-F | 231-25 |
| 72 625PN-F | 212-23 |
| 72 725PN-F | 195-23 |
| 72 824PN-F | 182-24 |
| 72 923PN-F | 168-25 |
| 721023PN-F | 157-25 |
| 721123PN-F | 144-24 |
| 721222PN-F | 132-23 |
| 73 121PN-F | 119-22 |
| 73 220PN-F | 107-19 |
| 73 320PN-F | 91-17 |
| 73 421PN-F | 73-16 |
| 73 520PN-F | 57-16 |
| 73 620PN-F | 34-16 |
| 73 719PN-F | 11-17 |
| 73 819PN-F | 229-19 |
| 73 918PN-F | 206-20 |
| 731018PN-F | 187-20 |
| 731117PN-F | 167-19 |
| 731220PN-F | 151-17 |
| 74 120PN-F | 138-15 |
| 74 220PN-F | 123-12 |
| 74 320PN-F | 108- 9 |
| 74 419PN-F | 94- 6 |
| 74 518PN-F | 78- 3 |
| 74 618PN-F | 60- 1 |
| 74 718PN-F | 41. 1 |
| 74 818PN-F | 22. 1 |
| 74 917PN-F | 1. 0 |
| 741016PN-F | 220- 1 |
| 741115PN-F | 220- 1 |
| 741215PN-F | 182. 0 |
| 75 115PN-F | 166. 2 |
| 75 215PN-F | 148. 4 |
| 75 315PN-F | 131. 6 |
| 75 415PN-F | 117. 8 |
| 75 514PN-F | 99.10 |
| 75 614PN-F | 80.12 |
| 75 713PN-F | 72.13 |
| 75 813PN-F | 47.14 |
| 75 912PN-F | 24.14 |
| 751011PN-F | 1.13 |
| 751110PN-F | 221.12 |
| 751210PN-F | 200.12 |
| 76 1 9PN-F | 182.12 |
| 76 2 9PN-F | 163.13 |
| 76 3 9PN-F | 145.14 |
| 76 4 8PN-F | 130.15 |
| 76 5 8PN-F | 112.16 |
| 76 6 7PN-F | 93.17 |
| 76 7 7PN-F | 77.18 |
| 76 8 7PN-F | 58.18 |
| 76 9 6PN-F | 39.19 |
| 7610 5PN-F | 17.18 |
| 7611 4PN-F | 235.17 |
| 7612 4PN-F | 217.17 |
| 77 1 4PN-F | 195.17 |
| 77 2 4PN-F | 176.17 |

Table 3. Sample output listing for Pioneer 10[a]

| Limit | Declination | Date | Week | DSS 11 | | DSS 12 | | DSS 14 | | DSS 42 | | DSS 51 | | DSS 61 | | DSS 62 | |
|---|---|---|---|---|---|---|---|---|---|---|---|---|---|---|---|---|---|
| | | | | Rise | Set | Rise | Set | Rise | Set | Rise | Set | Rise | Set | Rise | Set | Rise | Set |
| 0900 | −15 | 2/27/72 | 9 | 1154 | 2146 | 1134 | 2142 | 1203 | 2131 | 1703 | 0523 | 0112 | 1308 | 0436 | 1348 | 0416 | 1408 |
| 0418 | −32 | 3/27/72 | 13 | 0832 | 1524 | 0744 | 1548 | 0833 | 1537 | 1129 | 0109 | 2030 | 0826 | 0106 | 0758 | 0046 | 0806 |
| 0200 | −29 | 4/26/72 | 17 | 0558 | 1330 | 0514 | 1346 | 0559 | 1335 | 0911 | 2251 | 1812 | 0608 | 2236 | 0556 | 2216 | 0608 |
| 2306 | −25 | 5/25/72 | 21 | 0240 | 1108 | 0204 | 1108 | 0245 | 1101 | 0641 | 1957 | 1518 | 0314 | 1930 | 0314 | 1906 | 0334 |
| 2112 | −23 | 6/25/72 | 25 | 0038 | 0922 | 0006 | 0922 | 0043 | 0915 | 0455 | 1755 | 1324 | 0120 | 1724 | 0128 | 1708 | 0148 |
| 1930 | −23 | 7/25/72 | 30 | 2256 | 0740 | 2224 | 0740 | 2301 | 0733 | 0313 | 1613 | 1142 | 2338 | 1542 | 2346 | 1526 | 0006 |
| 1812 | −24 | 8/24/72 | 34 | 2142 | 0618 | 2110 | 0618 | 2147 | 0611 | 0151 | 1455 | 1024 | 2220 | 1432 | 2224 | 1412 | 2240 |
| 1648 | −25 | 9/23/72 | 38 | 2022 | 0450 | 1946 | 0450 | 2027 | 0443 | 0023 | 1339 | 0900 | 2056 | 1312 | 2056 | 1248 | 2116 |
| 1542 | −25 | 10/23/72 | 42 | 1916 | 0344 | 1840 | 0344 | 1921 | 0337 | 2317 | 1233 | 0754 | 1950 | 1206 | 1950 | 1142 | 2010 |
| 1424 | −24 | 11/23/72 | 47 | 1754 | 0230 | 1722 | 0230 | 1759 | 0223 | 2203 | 1107 | 0636 | 1832 | 1044 | 1836 | 1024 | 1852 |
| 1312 | −23 | 12/22/72 | 51 | 1638 | 0122 | 1606 | 0122 | 1643 | 0115 | 2055 | 0955 | 0524 | 1720 | 0924 | 1728 | 0908 | 1748 |
| 1154 | −22 | 1/21/73 | 3 | 1516 | 0008 | 1440 | 0008 | 1521 | 0001 | 1945 | 0837 | 0406 | 1602 | 0758 | 1614 | 0742 | 1634 |
| 1042 | −19 | 2/20/73 | 8 | 1348 | 2312 | 1324 | 2312 | 1357 | 2301 | 1837 | 0721 | 0254 | 1450 | 0634 | 1518 | 0614 | 1530 |
| 0905 | −17 | 3/20/73 | 12 | 1204 | 2144 | 1144 | 2140 | 1217 | 2129 | 1701 | 0537 | 0118 | 1314 | 0450 | 1350 | 0430 | 1406 |
| 0718 | −16 | 4/21/73 | 16 | 1012 | 2000 | 0956 | 1956 | 1025 | 1945 | 1517 | 0345 | 2330 | 1126 | 0258 | 1206 | 0238 | 1222 |
| 0542 | −16 | 5/20/73 | 20 | 0836 | 1824 | 0820 | 1820 | 0849 | 1809 | 1341 | 0209 | 2154 | 0950 | 0122 | 1030 | 0102 | 1046 |
| 0324 | −16 | 6/20/73 | 25 | 0618 | 1606 | 0602 | 1602 | 0631 | 1551 | 1123 | 2351 | 1936 | 0732 | 2304 | 0812 | 2244 | 0828 |
| 0106 | −17 | 7/19/73 | 29 | 0404 | 1344 | 0344 | 1340 | 0417 | 1329 | 0901 | 2137 | 1718 | 0514 | 2050 | 0550 | 2030 | 0606 |
| 2254 | −19 | 8/19/73 | 33 | 0200 | 1124 | 0136 | 1124 | 0209 | 1113 | 0649 | 1933 | 1506 | 0302 | 1846 | 0330 | 1826 | 0342 |
| 2035 | −20 | 9/18/73 | 37 | 2350 | 0902 | 2318 | 0902 | 2355 | 0851 | 0427 | 1715 | 1248 | 0044 | 1628 | 0104 | 1612 | 0120 |
| 1842 | −20 | 10/18/73 | 42 | 2156 | 0708 | 2124 | 0708 | 2201 | 0657 | 0233 | 1521 | 1054 | 2250 | 1434 | 2310 | 1418 | 2326 |
| 1642 | −19 | 11/17/73 | 46 | 1948 | 0512 | 1924 | 0512 | 1957 | 0501 | 0037 | 1321 | 0854 | 2050 | 1234 | 2118 | 1214 | 2130 |
| 1506 | −17 | 12/20/73 | 50 | 1804 | 0344 | 1744 | 0340 | 1817 | 0329 | 2301 | 1137 | 0718 | 1914 | 1050 | 1950 | 1030 | 2006 |
| 1348 | −15 | 1/20/74 | 3 | 1642 | 0234 | 1622 | 0230 | 1651 | 0219 | 2151 | 1011 | 0600 | 1756 | 0924 | 1836 | 0904 | 1856 |
| 1218 | −12 | 2/20/74 | 8 | 1504 | 0120 | 1440 | 0112 | 1513 | 0057 | 2033 | 0829 | 0434 | 1626 | 0738 | 1718 | 0726 | 1730 |
| 1048 | −9 | 3/20/74 | 12 | 1330 | 2358 | 1302 | 2358 | 1331 | 2339 | 1911 | 0647 | 0308 | 1456 | 0552 | 1556 | 0548 | 1608 |

[a]View periods 1972–1976.

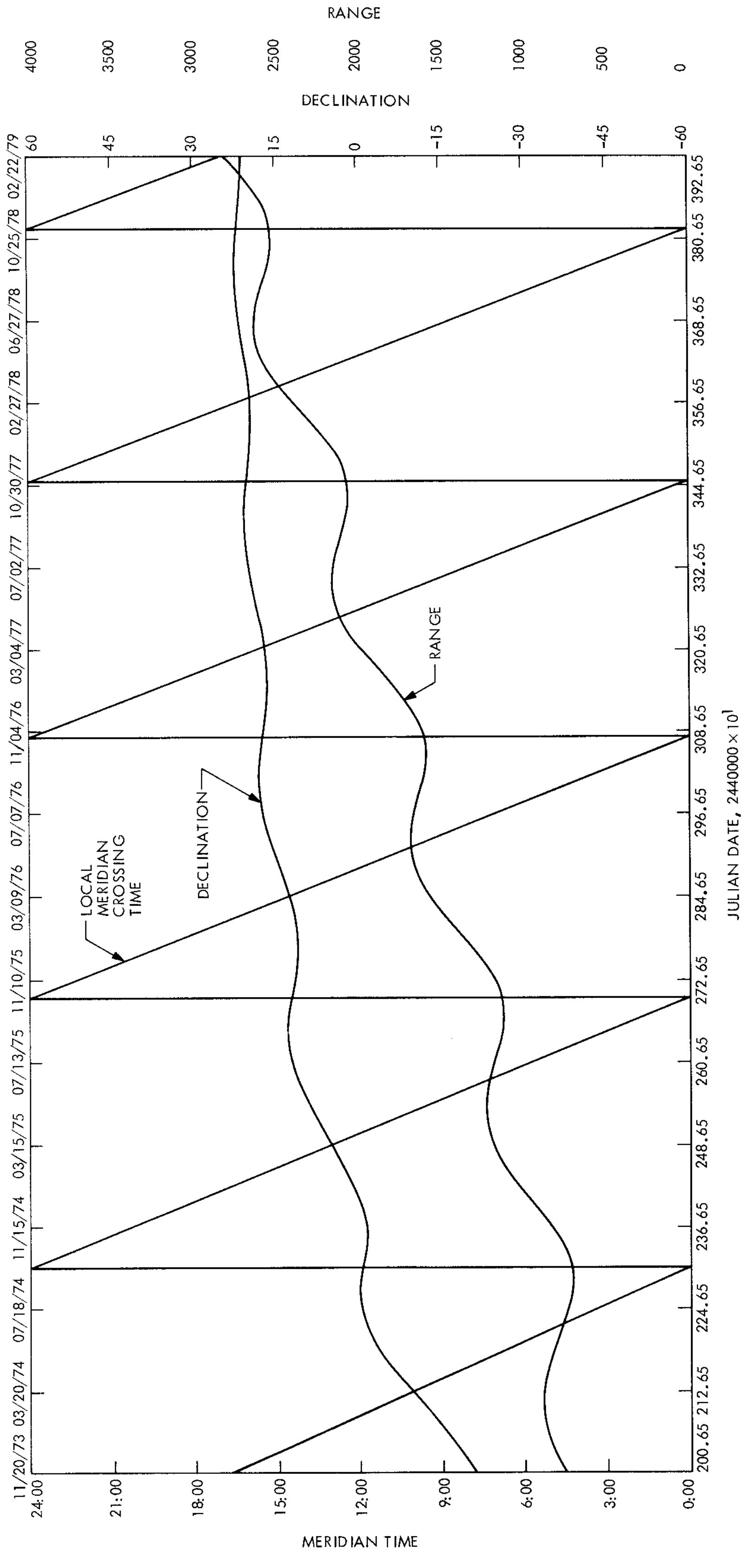


**Fig. 1. LMCT–declination–ranging plots**

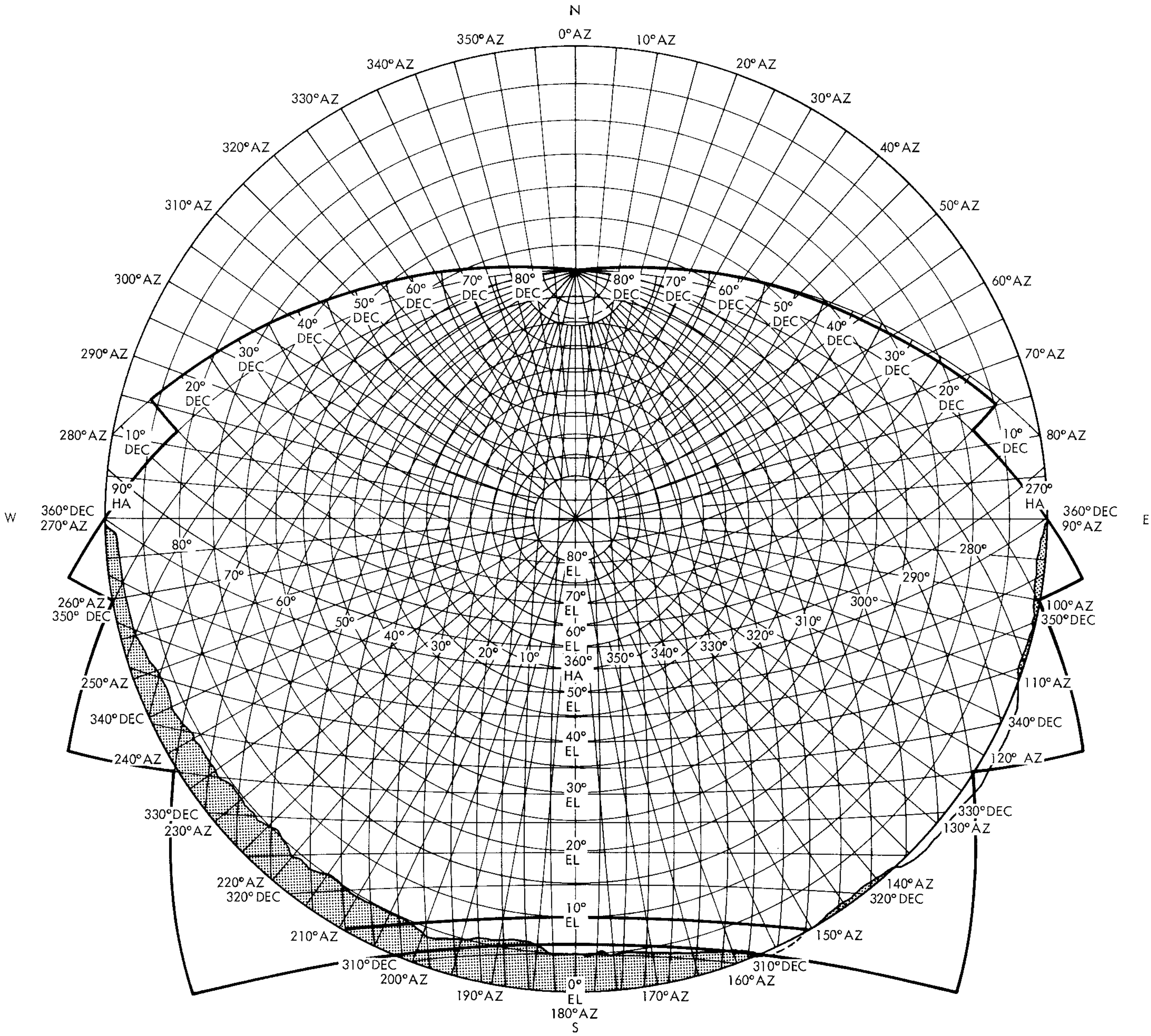


| ANTENNA LIMITS | | | | | |
|---|---|---|---|---|---|
| DEC | PRE | FINAL | HA | PRE | FINAL |
| DN | 082.590 | 083.560 | H1E | 267.560 | 266.840 |
| D2E | 015.072 | 013.958 | H2E | 270.942 | 270.050 |
| D3E | 352.958 | 351.176 | H3E | 276.066 | 275.008 |
| D4E | 334.870 | 333.850 | H4E | 290.668 | 290.076 |
| D2W | 015.072 | 013.958 | H1W | 095.162 | 096.012 |
| D3W | 352.958 | 351.176 | H2W | 088.978 | 089.486 |
| D4W | 334.870 | 333.850 | H3W | 083.818 | 084.702 |
| DS | 312.540 | 311.450 | H4W | 069.010 | 069.878 |

**Fig. 2. Sample stereographic projection**